Improvement in the Dynamic Behavior of the Microgrid using a Doubly Fed Induction Wind Generator

Bibhu Prasad Nanda [1] Himanshu Shekhar Maharana [2] Debswarup Rath [3]
Einstein Academy Of Technology And Management,
Bhubaneswar

***Abstract*—This paper describes a control approach applied on a doubly fed induction generator (DFIG) to provide both voltage and frequency regulation capabilities, and hence, an improvement in the dynamic behavior of a microgrid system. The microgrid system is assumed to be a portion of a medium voltage distribution feeder and is supplied by two distributed generation (DG) units, i.e., a gas turbine synchronous generator and a variable-speed wind turbine with DFIG. A control approach algorithm is proposed for the DFIG unit to improve both voltage and primary frequency controls. Two distinct operation modes, i.e., grid-connected and islanding mode, are used in the proposed approach for proper transfer from normal to islanding operation. Case studies are simulated based on both planned and unplanned islanding scenarios to evaluate the performance of the control approach. The study results show that the proposed control approach for DGs in the microgrid increase the microgrid system's dynamic performance, reduce frequency changes, and improve bus voltages regulation during islanding and autonomous operations.**

***Index Terms*—Distributed generation (DG), doubly fed induction generator (DFIG), frequency and voltage controls, islanding, microgrid.**

NOMENCLATURE

A_r	Area covered by the turbine blades.
C_{popt}	Optimal power coefficient.
d, q	First subscript indicates direct and quadrature axes quantities.
e_t	Terminal voltage of the DFIG.
K_{opt}	Optimal torque/speed constant of the Wind turbine.
L_m	Magnetizing inductance of the DFIG. L_s Stator leakage inductance of the DFIG.
P_{opt}	Optimal extraction power.
r, θ	Blade radius and pitch angle of the wind turbine.
R	Droop value of frequency-real power characteristic.
s, r	Second subscript indicates a stator and a rotor.
T_e , $T_{e\ opt}$	Electromagnetic and optimal electromagnetic torque.
λ_{opt}	Optimal tip speed ratio.
v_ω	Wind speed.
ρ	Air density.
ω_s , ω_r	Synchronous and rotor angular speed.
ω_t	Wind turbine rotor speed.

I. INTRODUCTION

Distributed power generation system is emerging as a complementary infrastructure to the traditional central power plants. This infrastructure is constructed on the basis of decentralized generation of electricity close to consumption sites using distributed generation (DG) sources [1]. The increase in DG penetration depth and the presence of multiple DG units in electrical proximity to one another have brought about the concept of the micro grid [2], [3]. A micro grid is defined as a cluster of DG units and loads, serviced by a distribution system, and can operate in the grid-connected mode, islanded (autonomous) mode, and ride-through between the two modes. The idea supporting the formation of the micro grid is that a paradigm consisting of multiple generators and aggregated loads is far more reliable and economical than a single generator serving a single load. Planned (intentional) islanding and autonomous operations of the micro grid supplied by local distributed energy resources (DERs) has recently attracted major utilities' interest worldwide [4], [5]. The concept can potentially improve reliability and supply security of the distribution network by reducing system downtime. It also allows the utility company to perform maintenance on upstream medium-voltage (MV)/high-voltage feeders without supply interruption of the low-voltage customers. The formation of an islanded micro grid, due to an islanding process, can be caused by disturbances, such as a fault, or as a result of intentional islanding events. After disconnection from the main grid, microgrid experiences frequency and voltage deviations. The amount of these deviations is highly dependent on: 1) the pre islanding operating conditions; 2) the type of the event that initiates islanding; and 3) the type of DG units within the micro grid. The micro grid is expected to remain operational after islanding and meet the corresponding load requirements during the autonomous operation. Transients and the small-

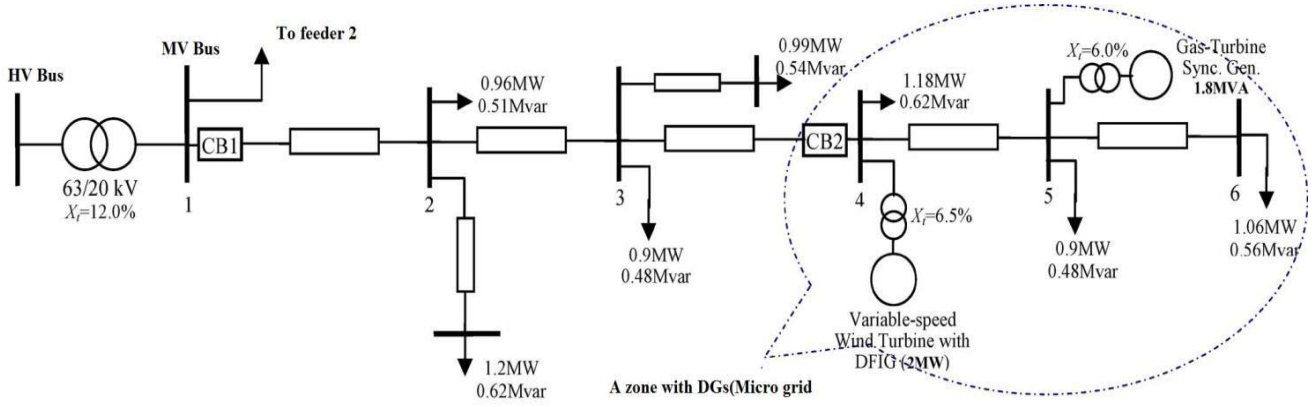

Fig. 1. Schematic diagram of the study system.

signal dynamic model of a micro grid including conventional and electronically interfaced distributed resources are investigated and presented in [6] and [7]. The wind-turbine-based DG unit is one of the fastest growing sources of power generation in the world mainly due to: 1) strong worldwide available wind resources; 2) environment friendly power generation source especially suitable for remote areas; and 3) rapid technological development [8]. The continuous trend of increase in the rate of DG connection and penetration depth of wind-turbine-based DG units can provoke several technical concerns and adverse impact on the operation of distribution systems [9]. Among the different wind energy conversion systems, double fed induction generators (DFIGs) are capable of providing the required capabilities without the need of large costs on the power electronics hardware, provided that adequate control strategies are added [10]. The control flexibility provided by the DFIG [19] electronic converter makes it possible to define various control strategies for participation in primary frequency control and voltage regulating support. In this paper, the developed dynamic model of a variable speed wind turbine with DFIG is employed to provide additional support to primary frequency control and voltage regulation of a micro grid. This can improve the dynamic behavior of a micro grid during islanding and autonomous mode operations. The proposed control approach consists of using an additional frequency control loop and a voltage regulating control loop, which are integrated into the rotor-side controller of a DFIG. To complete the control approach, a pitch control strategy is also included, and it dominates the power control for high wind speeds. In order to evaluate the effectiveness and advantages of the proposed control scheme, two types of disturbances, planned switching event (intentional islanding) and unplanned switching event (unintentional islanding), e.g., a short-circuit event on an upstream section of the feeder, are applied in a study system. The study system is designed and the corresponding digital computer simulation model is developed using MATLAB R2010 software package.

II. Study System Description

Fig. 1 shows a single-line diagram of a 20-kV local distribution feeder used to investigate possible micro grid operational scenarios. In this distribution system, the last section of feeder1 that consists of DG units and loads is capable of operating in islanded mode from the main grid. This section constitutes the micro grid system. This micro grid system includes two DG units. DG1 is a 1.8-MV · A conventional gas-turbine generator equipped with excitation and governor control systems. A full description of such a gas-turbine generator can be found in [11].

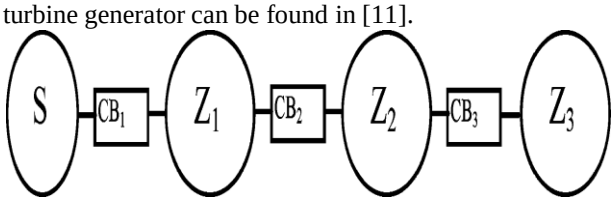

Fig. 2. Schematic diagram of a distribution system with the proposed zones.

DG2 represents a variable-speed wind turbine set with rated capacity of 2 MW, which is interfaced through a DFIG with rated capacity of 2.5 MV · A. The DG1 and DG2 parameters are given in the Appendix. The micro grid system is separated from the rest of the MV feeder by a circuit breaker.

III. ISLANDING DETECTION AND THE SYSTEM PROTECTION SCHEME

Under the regulation governing distribution system operation, an islanding scenario is permitted only for loads with dedicated generation units. As a result, DG units must be equipped with specific islanding detection and prevention schemes to disconnect the unit within 2 s of an islanding event [12]. However, in the future, to realize the full benefit of high DG penetration depth, the islanding operation of micro grids needs to be considered.

In the case of future micro grid applications, with the potential of islanding operation, a fast and reliable detection algorithm is required to effectively distinguish between an islanding condition and other types of disturbances. In this research, the islanding and formation of a micro grid is assumed to be detected within 100 ms (five cycles in 50 Hz). After detection, the islanding mode operation of the micro grid is activated by changing the DGs control mode. To consider the islanding operation of micro grids, a protection scheme in distribution network can be suggested as follows. The distribution system is divided into several zones in such a way that in each zone, there is no DG, or if there is any, balance of generation and consumption in that zone is possible regardless of the main grid and by using only the power generated by DGs that exist in that zone (micro grid concept) [13] (see Fig. 2).

In other words, the distribution system is divided into two categories: the first category includes those zones that have no DG and their loads are fully supplied through the main grid, and the second category includes those zones that have one or more DGs and are capable of operating in the islanded mode. The zones are interconnected using breakers with fast and consecutive open and close capabilities as well as receiving remote command. Besides, these breakers must be equipped with synchro-check relays, to be able to maintain zones synchronization when it is needed to connect two island zones.

Using an online fault diagnosis algorithm and coordination of protection devices, such as recloser and fuses and remote control of breakers in the system, the faulted part of the network can be detected and isolated from the rest of the grid. In this scheme, out-of-phase (asynchronous) reclosure will not occur. This is an important feature, because the out-of-phase reclosure can impose heavy damages on distribution system devices.

Fig. 3. Schematic representation of the proposed control approach

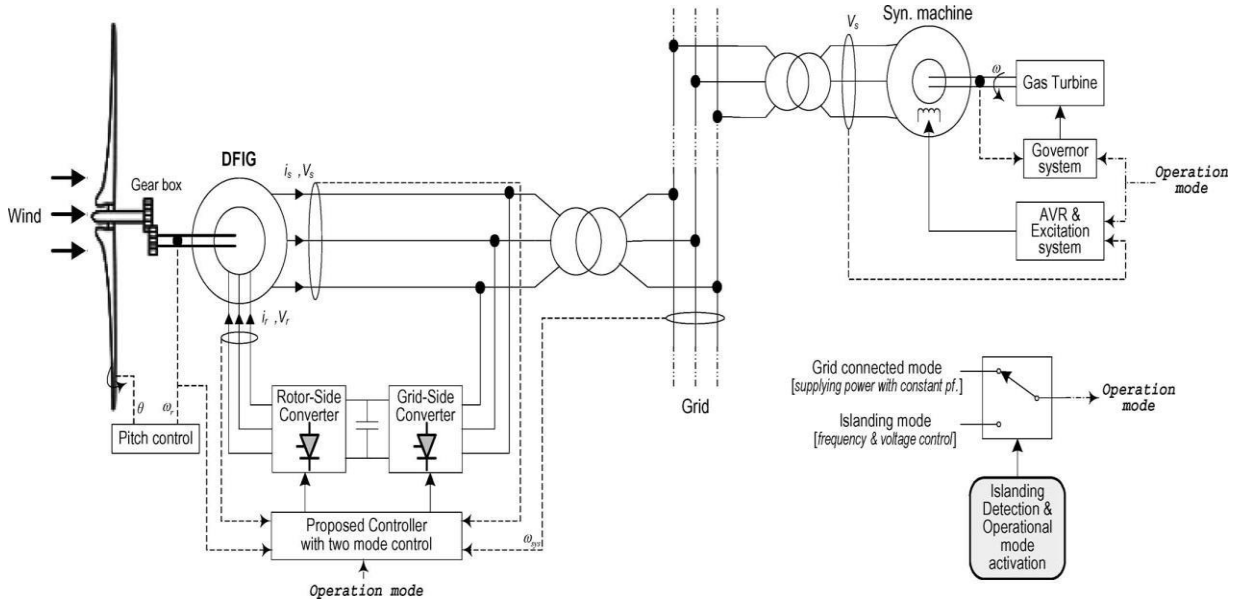

IV. MICROGRID OPERATIONAL MODES

In the proposed microgrid system (Fig. 1), the islanding incident that results in the islanding operation can be due to either a planned (intentional) or an unplanned (unintentional) switching event. In the case of planned islanding operation, appropriate microgrid load sharing among the DG units and the main grid may be scheduled prior to islanding. Thus, the islanding process results in minimal transients and the micro grid continues to operate. An unplanned islanding and micro grid formation is due to either a fault and its subsequent switching events or some other unexpected switching process. Prior to islanding, the operating conditions of the micro grid could be widely varied, e.g., the DG units can share load in various manners. In the proposed system, planned islanding and unplanned islanding due to a fault in upstream of the microgrid will be investigated. In the grid-connected mode, DG units are expected to supply their local demand or operated in their optimal operating point from efficiency point of view. This can be due to the economics aspects. Also to avoid interference with the voltage regulator devices in the network, DGs normally operate at constant power factor (close to unity) and do not control the grid voltage actively.

In the study system of Fig. 1, DG1 generates constant real power output (close to unity power factor) and DG2 delivers maximum power extracted from the wind with unity power factor (DFIG capability). In this mode, the grid acts as a slack bus that dominantly supports the real/reactive power requirements during transients or due to the power fluctuations caused by DG2, and also stabilizes the frequency.

In the islanding-mode operation, fast and flexible real/reactive power control strategies are required to minimize dynamics of the system and damp out transient power oscillations where no infinite source of power is available. In the proposed system, DG1 is equipped with excitation and governor systems. After islanding detection, DG1 switches to islanding mode by regulating its terminal voltage at a reference value, e.g., 1 per unit (p.u.), through excitation system [using automatic voltage regulator (AVR)] and by controlling deviations in the generator speed through a governor system that is implemented based on a frequency-active power relation (droop characteristic) and a frequency restoration loop (using an integrator). Also, DG2 switches to islanding mode by contributing to primary frequency control and regulating its terminal voltage through both q- and d-axis of rotor currents.

The proposed algorithm and the control approach, in general, are illustrated in Fig. 3.

V. SYSTEM MODEL

The MATLAB R2010 software package is used to develop a time-domain simulation model of the study system of Fig. 1. The component models used for simulation are as follows. The main grid (63-kV side of the distribution substation) is represented by a 63- kV three-phase voltage source with the short-circuit capacity of 1600 MV · A and X/R ratio of 15. The distribution substation 63-/20-kV transformer is represented as a linear transformer with appropriate winding connections (see Fig. 1). Each feeder is represented as a three-phase overhead line with lumped RL elements per phase or a cable with π equivalent circuits (R, L, and C elements) per phase. DG1 is modeled as a single-mass machine. The machine electrical system is represented in the d–q–o frame with two rotor windings on each axis. The excitation and governor systems of the machine are also included in the model.

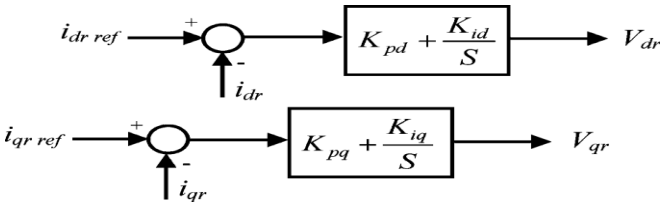

Fig. 4. PI controllers of the rotor-side converter.

DG2 is modeled as a variable-speed wind turbine with a DFIG. The mechanical power generated by the rotor is converted into electrical power using a DFIG. In the doubly fed (wound rotor) induction generator, the stator winding is coupled directly to the grid. The rotor winding is connected to a back-to-back voltage source converter. Speed controller, primary frequency controller, pitch angle controller, and terminal voltage regulator are included in the model, and described in the following sections.

A. Variable-Speed Wind Turbine With DFIG

The equations describing a doubly fed induction machine can be found in [14]. When modeling the DFIG, the generator convention will be used, which means that the current direction is toward the output instead of inputs. The generator equations in a d–q reference frame used in this research is given in [15]. Note that the d–q reference frame is rotating at synchronous speed with the q-axis 90◦ ahead of the d-axis. The position of the d-axis coincides with the maximum of the stator flux, which means that V_{qs} equals the terminal voltage e_t and V_{ds} equals zero

[15]. For simplicity, dynamic phenomena and switching transients in a back-to-back voltage source converter are neglected. Instead, the rotor-side converter is modeled as a controllable voltage source, and the grid-side converter is modeled as a controllable current source. The rotor-side converter is used to control speed and both active and reactive power outputs through V_{qr} and V_{dr} components obtained from two separate sets of PI controllers, as shown in Fig. 4. To consider the rated capacity of the back to-back converter, the limits are imposed on both rotor d- and q-axis currents.

The grid-side converter is used to take into account the balance of active power between the rotor and the grid.

B. Maximum Power Extraction and Speed Controller

The maximum (optimal) power obtained from a given wind speed is commonly expressed by the following equation:

$$P_{opt} = 0.5\rho C_{popt}(\lambda_{opt}, \theta) A_r v_\omega^3 \quad (1)$$

with C_{popt} being the optimal power coefficient of the wind turbine for a given wind speed, A_r (in square meters) the effective area covered by the turbine blades, v_w (in meters per second) the wind speed, and ρ (in kilograms per cubic meter) is the air density. The calculation of the optimal power coefficient

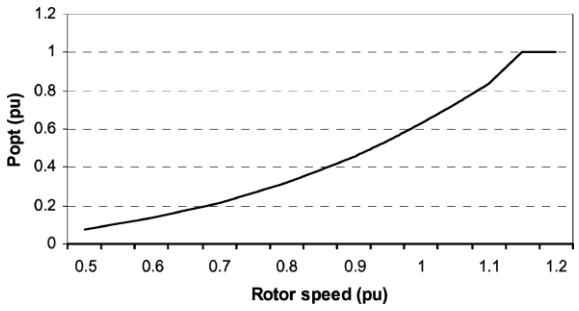

Fig. 5. Optimal extraction power curve.

C_{popt} can be obtained from the following function [15]:

$$C_{popt}(\lambda_{opt},\theta) = 0.22\left(\frac{116}{\lambda i} - 0.4\theta - 5\right) e^{-\frac{12.5}{\lambda i}}$$

$$\frac{1}{\lambda i} = \frac{1}{\lambda + 0.08\theta} - \frac{0.035}{\theta^3 + 1}$$

The optimal tip speed ratio is defined as

$$\lambda opt = \frac{\omega}{v_\omega}$$

where r (in meters) is the blade radius and ω_{topt} is the optimal wind turbine rotor speed (in radians_ mechanical per second) for a given wind speed. From (1) and (4), an optimum (maximum) power value P_{opt} can be obtained as a function of the shaft speed, referred to as the generator side of the gearbox, as follows:

$$P_{opt} = K_{opt}\omega_r^3 \quad (5)$$

Where $K_{opt} = (\rho/2)(Cp_{opt}/\lambda_{opt})\pi r^5$, $\omega_r = (P/2) G\omega_t$, P being the number of poles and G the gear ratio. From (5), the wind turbine predefined optimal extraction power curve can be established for a given K_{opt} associated to a fixed blade angle. In this research, K_{opt} is defined for a fixed blade angle equal to 0◦ . In Fig. 5, the maximum power extraction curve adopted for a variable-speed wind turbine is shown. The speed controller is controlling the electromechanical torque (T_e). The reason for such control is that the torque is directly dependent on the quadrature component of the rotor current (i_{qr}), when stator resistant is neglected [16]. The following relation between torque and i_{qr} holds, in which e_t is the terminal voltage:

$$T_e = \frac{-L\ e}{L + Lm}\ i_{qr} \quad (6)$$

From (5), the relation between the electromechanical torque and the rotor speed can be derived as follows:

$$T_{e\,opt} = K_{opt}\omega_{r2} \quad (7)$$

From (6) and (7), the rotor speed controller is implemented by measuring the actual rotor speed and then the value of i_{qr} needed to realize the desired electromechanical torque is calculated. The resulting i_{qr} ($i_{qr\ ref}$) is fed into theDFIG through V_{qr} component using a PI controller (see Fig. 6). This control algorithm is applied up to the maximum mechanical power of the turbine.

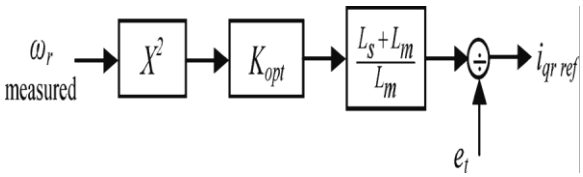

Fig. 6. Rotor speed controller (maximum power extraction).

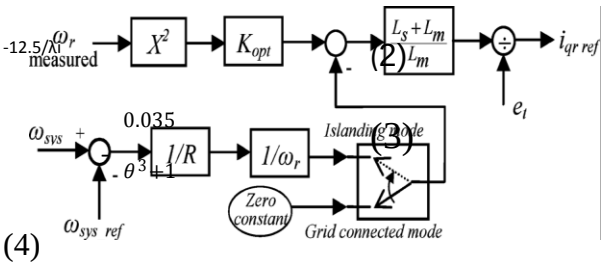

Fig. 7. Integrated active power and primary frequency control of the DFIG.

C. Primary Frequency Control

Variable-speed wind turbines are controlled to capture as much power as possible from the wind. However, the large blades of the turbine give this type of DG unit a significant inertia. The kinetic energy stored in their inertia gives the turbine the possibility to support primary frequency control for a short period. One particular advantage of variable- speed wind turbines is that unlike thermal or gas turbine power plants, they can increase their output power almost instantaneously [17]. This is an important feature, especially for a microgrid system when it goes to islanding-mode operation. The primary frequency control integrated into the rotor- side speed (active power) control loop is similar to the one usually used in a synchronous generator. In this case, the droop (characterized by a regulation R, expressed in p.u. in the system base) is used to produce a change in the active power injected by the DFIG when a system frequency variation occurs. The active power increment is therefore proportional to the system frequency variation and is defined as follows:

$$Q_{grid}=-\left(\frac{Lm}{L+Lm}\right)$$

$$P_{injected}=P_{ref}-\left(\frac{1}{R}\right)(\omega_{sys}-\omega_{sys\text{-}ref}) \quad (8)$$

This generated active power requires a new operating point of theDFIG. The primary frequency control that integrated into the rotor-side speed control loop is implemented by converting the required active power to equivalent electromechanical torque (see Fig. 7). Note that this feature (primary frequency control) is activated when an islanding condition occur. The variable ω_{sys} is obtained from the grid connection bus voltage of the DFIG using a phase lock loop (PLL).

D. Pitch Control

For wind speeds below maximum rated speed (according to the operational optimal power curve), the input reference electromechanical torque to the active power (rotor speed) control loop in DFIG follows (6) and (7), as discussed in the previous section. However, for wind speed larger than the maximum rated speed, the blade pitch regulation dominates the control and limits the energy captured from the turbine. In this case, the pitch control will control the rotor speed and operate until the wind cutoff speed limit is reached .A typical pitch control can be found in [15]. The input speed reference for a pitch control is defined according to if $P_{mec} > P_{max}$, and then $\omega_{r\text{-}ref} = (P_{max}/T_{mec})$.

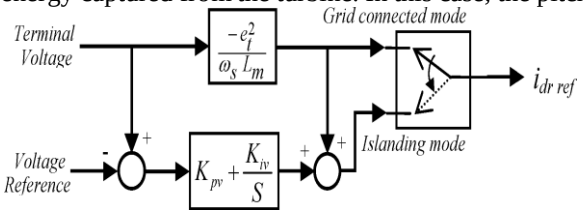

Fig. 8. Terminal voltage controller of the DFIG.

E. Reactive Power Control and Terminal Voltage Regulator

A variable-speed wind turbine with DFIG has the capability to control its terminal voltage. It is an important feature, especially for a micro grid islanding operation. By this feature, the DFIG can contribute the reactive power management and voltage regulation of the microgrid. A terminal voltage controller is being developed here. It can be applied in two operation modes of a microgrid (grid- connected mode and islanding operation mode). When stator resistance is neglected, the reactive power generated by the wind turbine is directly dependent on i_{dr} [16]. It can be shown that the relation between the reactive power generated and i_{dr} is as follows:

$$)(i_{dr,magn}+i_{dr,ge}\quad\frac{1}{\omega\ (L+Lm)}\quad)\quad(9)$$
$$_n)-e_t^2($$

where the direct component of the rotor current has been split into a part that magnetizes the generator, $i_{dr,magn}$, and a part that determines the net reactive power exchange with the grid, $i_{dr,gen}$. The direct component of the rotor current necessary to magnetize the generator itself has the following value:

$$^2\left(\frac{1}{\omega sLm}\right) \quad (10)$$

The value of $i_{dr,gen}$ determines whether the net reactive power is generated or consumed. The terminal voltage will increase when more reactive power is delivered to the grid. The voltage controller should have the following features.

1) In the grid-connected mode operation of the microgrid, the DFIG should be operated at unity power factor.

2) Terminal voltage of the DFIG should be adjusted appropriately when the microgrid switches to islanding mode.

A voltage controller that satisfies the aforementioned features is proposed and depicted in Fig. 8. From Fig. 8, it can be seen that during the grid-connected mode of operation, $i_{dr,ref}$ provides the required magnetization current for the DFIG. Also, in the islanding mode of operation, in addition to providing the required magnetizing current, the PI controller regulates $i_{dr,ref}$ in a way that it provides the required reactive power.

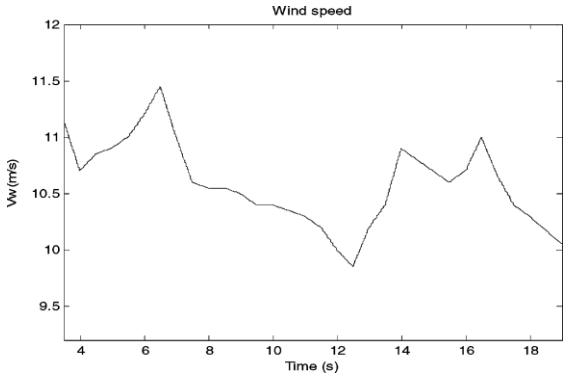

Fig. 9. Real wind speed pattern.

VI. TEST CASES AND SIMULATION RESULTS

Two case studies have been demonstrated to show the ability of DG controllers (especially for a DFIG) to continue the micro grid operation during separation and in the islanded mode. Case studies are chosen to illustrate both the steady-state and dynamic responses to the changes in the system operating point.

A. Unplanned (Unintentional) Islanding Event

In this case study, it is assumed that an unplanned islanding event of the microgrid system takes place due to a fault occurrence in the upstream section of the MV feeder. Prior to islanding, the operating conditions of the system are the same as those of the planned islanding case.

At t = 4.0 s, a three-phase fault occurs on bus 2 in the upstream section of the supply MV feeder. Considering the proposed system protection scheme, after about 150 ms, the fault is diagnosed, and an opening command is issued for CB2 from a distribution network operator (DNO). After opening the CB2, synchronous reclosing operation of the upstream section can be made available by CB1, and also islanding operation of the microgrid system will be allowed. The islanding phenomena is detected 100 ms after CB2 opens, i.e., at t = 4.25 s. At this moment, the operation mode of DG units in the microgrid system switches to the islanding mode. Fig. 11 shows the system transients during the unplanned islanding scenario.

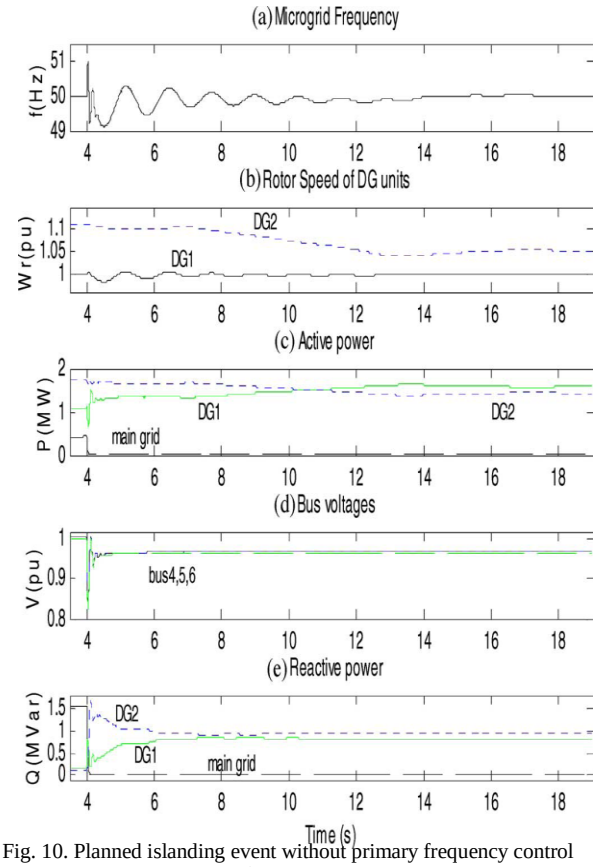

Fig. 10. Planned islanding event without primary frequency control of the DFIG.

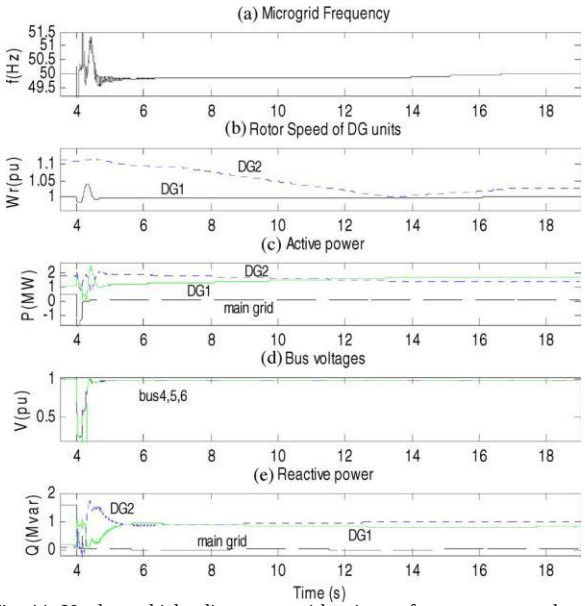

Fig. 11. Unplanned islanding event with primary frequency control of the DFIG.

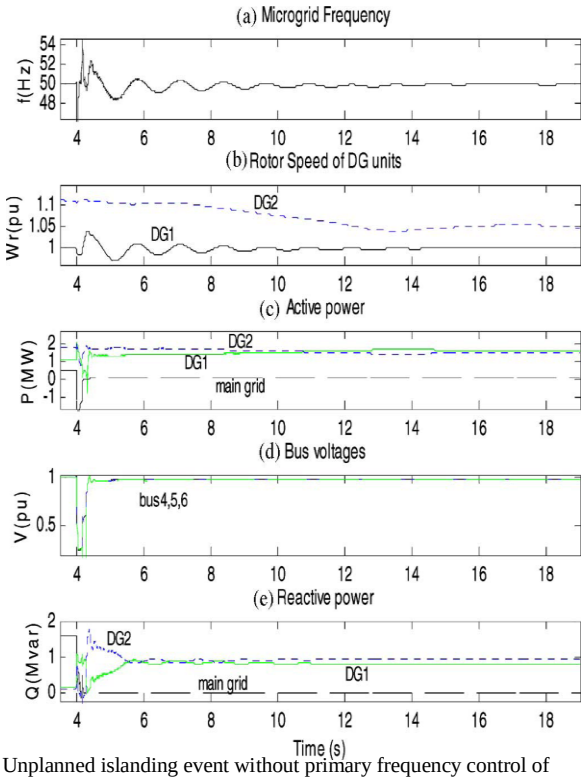

Fig. 12. Unplanned islanding event without primary frequency control of the DFIG.

During the fault, bus voltages drop severely [see Fig. 11(d)]. After the islanding detection, fast control actions of the DG units' terminal voltage controllers eventually return the voltages to their normal range.

Fig. 12 illustrates the system response when the DFIG primary frequency control is disabled. From Figs. 11 and 12, it is observed that the primary frequency control responds quickly and helps to improve the system frequency response slightly.

A better damping performance is obtained for the case where DFIG has a primary frequency control capability, as shown in Fig. 11(a), because after islanding detection, the DFIG participating in the primary frequency control leads to an increase

in active power injection. This fact makes it possible for DG1 (synchronous generator unit) to respond by injecting less active power into the microgrid, thereby improving the system frequency smoothly. It can be seen that when power increases, the DFIG rotor active power also increases, and consequently, the rotor speed tends to fall a little more after islanding detection balancing the total active power (stator plus rotor active power) injected by the DFIG, as illustrated in Figs. 11(b) and 12(b).

B. Planned (Intentional) Islanding Event

The objective of this study is to investigate dynamic behavior of the microgrid with DGs due to a planned islanding scenario. Prior to islanding, DG1 supplies 1.3 MW/0.05 Mvar (close to unity power factor) and the difference between the power generated by DG2 and the load demand of 3.14 MW/1.63 Mvar is imported from the grid (0.45 MW/1.57 Mvar). DG2 is operated at unity power factor, and a real wind pattern [18] with average wind speed of 10.3 m/s, as shown in Fig. 9, was used as input to the wind turbine. In this situation, about 86% of the total load in micro grid is supplied by DG units, and the rest is imported from the main grid. Both the gas-turbine synchronous generator unit (DG1) and the variable-speed wind turbine with DFIG unit (DG2) use a 5% droop value (in each machine base). At t = 4.0 s, the microgrid is disconnected from the main grid by initiating an intentional islanding command that opens CB2 in Fig. 1. Fig. 13 shows the system transients due to the planned islanding event. Fig. 13(d) illustrates that the bus voltages recovered to its normal range in 70 ms. It is due to the contribution of both DFIG terminal voltage controller and excitation system of the synchronous generator unit in reactive power compensation and voltage regulation of the islanded network (the micro grid system). Fig. 13(c) also shows power sharing of the DG units after islanding based on power control strategy of the DG units in micro grid. DG1 adjusts its real power output through the action of its governor, according to its dynamic response time. Also, the restoration of microgrid frequency is accomplished by DG1 through frequency restoration control loop (integral frequency control) that integrated in its governor system.

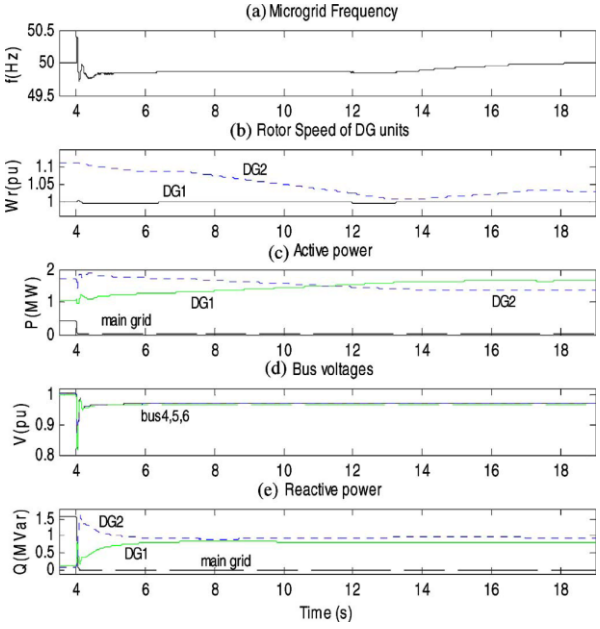

Fig. 13. Planned islanding event with primary frequency control of the DFIG.

DG2 supports the primary frequency control of the islanded system (microgrid) through its proposed controller. Hence, the frequency deviation in the islanded system is acceptable, and it can be seen that the microgrid system frequency restores to the reference value of 50 Hz [see Fig. 13(a)]. During the islanding operation, the real power output of DG1 varies based on the changes in the output power of DG2 due to variation in the wind power that changes the speed of synchronous generator unit [see Fig.
13(b)]. Fig. 10 shows the case that primary frequency control capability of the DG2 is deactivated. From Figs. 13 and 10, it is clear that due to primary frequency control feature of the DG2 unit, an improved frequency control of the microgrid can be achieved. The results of this case study indicate that the proposed DFIG controllers can contribute to both voltage and frequency controls of a microgrid during separation and islanding operation. This leads to a good dynamic behavior of the microgrid during and subsequent to a planned islanding event.

VII. CONCLUSION

In this paper, the impact using a DFIG with capability to contribute to primary frequency control and terminal voltage regulation in a microgrid system was addressed. Two control modes were adopted for DGs in a microgrid system, and both planned and unplanned islanding scenarios were examined to evaluate the control approach. The microgrid is supplied by two DG units, i.e., a synchronous machine and a variable-speed wind turbine with DFIG technology. The latter unit includes both voltage and primary frequency controls with a fast response time. A detailed description of the applied control approach was provided and discussed. The simulation results show that the proposed controllers for DFIG can lead to a better dynamic behavior of the microgrid when islanded from the main grid and operate in islanding mode. It was shown that having a variable-speed wind turbine with DFIG in a microgrid participating in the frequency and voltage controls may improve the microgrid system's dynamic performance, reducing the frequency changes following disturbances that are subsequent to islanding.

APPENDIX

A. DG1 (Gas-Turbine Synchronous Generator) Parameters

1) Synchronous machine characteristics:

S_n = 1.8 MV · A; V_n = 11 kV;
X_d = 1.56 p.u.;
$X_{\_d}$ = 0.29 p.u.; $X_{\_\_d}$ = 0.17 p.u.; X_q = 1.07 p.u.; $X_{\_q}$ = 0.35 p.u.;
$X_{\_\_q}$ = 0.17 p.u.; X_l = 0.055 p.u.; $T_{\_d}$ = 3.5 s;
$T_{\_\_d}$ = 0.035 s; $T_{\_\_q}$ = 0.037 s;
R_s = 0.0036 p.u.; H = 1.04 s.

2) AVR parameters: K_A = 400, T_A = 0.02 s.

3) Turbine-governor total time constant: about 450 ms.

B. DG2 (Variable-SpeedWind TurbineWith DFIG) Parameters

1) Wind Turbine characteristics:

P_n = 2 MW;
number of blades = 3;
rotor diameter = 80 m;
air density = 1.255 kg/m3 ;
gear box ratio = 1:85;
inertia time constant = 3.5 s;
nominal wind speed = 12 m/s; cut-in wind speed = 4.5 m/s; cutoff wind speed = 25 m/s.

2) DFIG parameters:

S_n = 2.5 MV · A; V_n = 0.69 kV;
R_s = 0.01 p.u.;
X_s = 0.1 p.u.; R_r = 0.01 p.u.; X_r = 0.08 p.u.; X_m = 3.0 p.u.;
number of poles = 4;
ω_s = 1500 r/min.

C. Control parameters:

K_{opt} = 0.628;K_{pd} = K_{pq} = 0.5,K_{id} = K_{iq} = 100;
K_{pv} = 0.1, and K_{iv} = 100.

It should be noted that the parameters of PI controllers are obtained based on the trial-and-error approach. Different values for different system conditions were investigated, and finally, the proposed values were selected.

REFERENCES

[1] M. W. Davis, "Distributed resource electric power systems offer significant advantages over central station generation and T&D power systems, part I," in Proc. 2001 IEEE Transmiss. Distrib. Conf. Expo., pp. 54– 61.
[2] N.D.Hatziargyriou and A. P. S. Meliopoulos, "Distributed energy sources: Technical challenges," in Proc. 2002 IEEE PESWinter Meeting, pp. 1017– 1022.
[3] C. L. Smallwood, "Distributed generation in autonomous and nonautonomous microgrid," in Proc. 2002 IEEE Rural Elect. Power Conf., pp. D1-1–D1-6.
[4] H. You, V. Vittal, and Z. Yang, "Self-healing in power systems: An approach using islanding and rate of frequency decline-based load shedding," IEEE Trans. Power Syst., vol. 18, no. 1, pp. 174–181, Feb. 2002.

[5] R. Fulton and C. Abbey, "Planned islanding of 8.6 MVA IPP for BC Hydro system reliability," in Proc. 2004 First Int. Conf. Integr. RE DER, pp. 1–9.
[6] F. Katiraei, M. R. Iravani, and P. W. Lehn, "Micro-grid autonomous operation during and subsequent to islanding process," IEEE Trans. Power Del., vol. 20, no. 1, pp. 248–257, Jan. 2005.
[7] F. Katiraei, M. R. Iravani, and P. W. Lehn, "Small- signal dynamic model of a microgrid including conventional and electronically interfaced distributed resources," IET Gener. Transmiss. Distrib., vol. 1, no. 3, pp. 369– 378, May 2007.
[8] The European Wind Energy Association (EWEA). (1999). Green peace and wind industry unveil global energy blue print [Online]. Available: http://www.ewea.org/src/press.htm
[9] S. K. Salman and A. Teo, "Windmill modeling consideration and factors influencing the stability of a grid- connected wind power-based embedded generator," IEEE Trans. Power Syst., vol. 18, no. 2, pp. 793–802, May 2003.
[10] J. Ekanayake and N. Jenkins, "Comparison of the response of doubly fed and fixed-speed induction generator wind turbines to changes in network frequency," IEEE Trans. Energy Convers., vol. 19, no. 4, pp. 800–802, Dec. 2004.
[11] W. J. Rowen, "Simplified mathematical representations of heavy duty gas turbines," ASME J. Eng. Power, vol. 105, pp. 865–869, 1983.
[12] IEEE Standard for Interconnecting Distributed Resources with Electric Power Systems, IEEE Standard 1547, Jul. 2003.
[13] S. M. Brahma and A. A. Girgis, "Development of adaptive protection scheme for distribution systems with high penetration of distributed generation," IEEE Trans. Power Del., vol. 19, no. 1, pp. 56–63, Jan. 2004.
[14] S. A. Papathanassion and M. P. Papadopoulos, "Dynamic behavior of variable speed wind turbines under stochastic wind," IEEE Trans. Energy Convers., vol. 14, no. 4, pp. 1617–1623, Dec. 1999.
[15] J. G. Slootweg, H. Polinder, and W. L. Kling, "Dynamic modeling of a wind turbine with doubly fed induction generator," in Proc. 2001 IEEE Power Eng. Soc. Summer Meeting, pp. 644–649.
[16] S. Heier, Grid Integration ofWind Energy Conversion Systems. Chicester, U.K.: John Wiley, 1998.
[17] H. Knudsen and J. N. Nielsen, "Introduction to the modeling of wind turbines," inWind Power in Power Systems, T.Ackerman, Ed. Chicester, U.K.: Wiley, 2005, pp. 525–585.
[18] Database of wind characteristics located at DTU, Denmark. (2006). [Online]. Available: http://www.winddata.com
[19] Parida R.N, Bibhu Prasad Nanda,,J.N Mishra," Sensorless Vector Control of Induction Generators for Variable-Speed Wind Turbines using Micro-2407" Energy and Power Engineering(Scientific Research publishing)July, 2012, Vol 4, No 4.pp 248-254.